

Phase Equilibria of (Pyrrole + Benzene, Cyclohexane, and Hexane) and Density of (Pyrrole + Benzene and Cyclohexane) Binary Systems[†]

Urszula Domańska* and Maciej Zawadzki

Department of Physical Chemistry, Faculty of Chemistry, Warsaw University of Technology, Noakowskiego 3, 00-664 Warsaw, Poland

The phase diagrams of pyrrole with benzene, cyclohexane, and hexane have been measured at ambient pressure by a dynamic method in a range of temperatures from (240 to 315) K. The simple eutectic system was observed with complete miscibility in the liquid phase for benzene. An immiscibility gap has been observed in the systems of {pyrrole (1) + cyclohexane or hexane (2)}. The upper critical solution temperatures (UCSTs) were observed for these two systems at (285.2 and 314.2) K for cyclohexane and hexane, respectively. The diagrams of phase equilibria have been correlated using the Wilson and the nonrandom two-liquid (NRTL) equation. The isothermal densities of pyrrole as a function of pressure was measured. Densities and excess molar volumes, V_m^E have been determined for pyrrole with benzene and cyclohexane over temperature range (298.15 to 338.15) K and ambient pressure. The densities of {pyrrole (1) + hexane (2)} mixture was not determined because of the problem of two phases up to 314.2 K. The temperature and composition dependences were described by linear or polynomial correlation. Excess molar volumes were calculated and correlated by the Redlich–Kister polynomial expansion. These systems exhibit negative excess molar volumes, V_m^E . Volume expansivity, α , and excess volume expansivity, α^E , were described in functions of temperature and composition. Our experimental data of V_m^E were used for the description of the excess molar enthalpy, H_m^E , for these systems with the Prigogine–Flory–Paterson (PFP) model. Negative V_m^E and H_m^E observed in these systems are probably attributed to the π – π interactions between the aromatic rings of pyrrole and benzene for the {pyrrole (1) + benzene (2)} mixture and by the high packing effects for the {pyrrole (1) + cyclohexane (2)} mixture.

Introduction

The experimental solid–liquid phase equilibria (SLE) and liquid–liquid phase equilibria (LLE) measurements of model compound as pyrrole are essential to process design and optimization. Pyrrole has unique physical and chemical properties and is used in the many laboratories as an entrainer in different chemical and manufacturing extracting processes.^{1–6} The immiscibility of pyrrole with water makes this compound ready to use in extraction processes from water.¹ The knowledge about density, excess molar volumes, or enthalpies and thermodynamic properties including phase equilibria is necessary to design any process involving pyrrole on an industrial scale.¹ Monte Carlo simulations were carried out to compute the vapor–liquid equilibria (VLE) of pyrrole between other aromatic compounds.² High-pressure phase equilibria of pyrrole with carbon dioxide was measured as an important compound in the enzymatic reactions.^{3,4} Ternary LLE were measured for pyrrole + hexadecane + nitrogen compound as information in the possible extraction of sulfur compounds from vehicle diesel.^{5,6}

All new data of phase equilibria are useful for determining parameters for group contribution models. Pyrrole may be used for determining the parameters of the $\text{NH}_{(\text{arom})}$ group existing in pyrrole and in the imidazoles. The first model connected with the imidazoles was made by us with the group contribution method DISQUAC.⁷ DISQUAC interaction parameters for the contacts present in the solution with aliphatic hydrocarbons,

aromatic hydrocarbons, and for the amine/hydroxyl contacts from the solutions with hydrocarbons and alcohols have been determined.⁷ Unfortunately, it was impossible to describe the LLE in many of the binary systems measured by us earlier. We hope that the new $\text{NH}_{(\text{arom})}$ group coming from pyrrole will improve the description, not only of pyrrole, but also of imidazoles. This may be useful for a subsequent study of imidazolium-based ionic liquid mixtures using DISQUAC. Imidazolium-based ionic liquids are extremely important for new technologies.^{8–13} On the other hand, the modified UNIFAC(Do) group interaction parameters were determined for the imidazolium bis{(trifluoromethyl)sulfonyl}imides with alkanes, alkenes, cyclic hydrocarbons, and alcohols, giving promising results in the prediction of VLE, activity coefficients at infinite dilution, and excess molar enthalpies.^{14–16}

It was proven by the measurements of the activity coefficient at infinite dilution, γ_{13}^∞ , that the imidazolium-based ionic liquids with the thiocyanate anion $[\text{SCN}]^-$ have high extraction efficiencies for the hexane/thiophene or hexane/benzene separation problems.^{11,12} These are very promising results for the separation of sulfur from mixtures of industrial importance and for the separation of alkanes from aromatics, which needs more thermodynamic information and the possibility of prediction of different mixtures. Thus, the interaction parameters for similar compounds are of industrial importance.

The present study is the first of the series of characterization of the (pyrrole + organic solvent) binary mixtures. This work is concerned with the investigation of phase equilibria of mixtures containing benzene, cyclohexane, and hexane and

[†] Part of the “Workshop in Memory of Henry V. Kehiaian”.

* Corresponding author. Telephone: + 48-22-6213115. Fax: + 48-22-6282741. E-mail: ula@ch.pw.edu.pl.

Table 1. Physicochemical Characterization of Pure Substances^a

name	M g·mol ⁻¹	$T_{\text{fus}}^{\text{exp}}$ K	$T_{\text{fus}}^{\text{lit}}$ K	$\Delta_{\text{fus}}H^{\text{lit}}$ kJ·K ⁻¹	$10^4 \alpha^{\text{exp}}$ K ⁻¹	κ_T^{exp} GPa ⁻¹	$\rho^{298.15,\text{exp}}$ g·cm ⁻³
pyrrole	67.09	249.55	248.38 ^b	7.91 ^c	8.96	0.608	0.96554
benzene	78.11	278.61	278.68 ^d	9.866 ^d	12.2	0.967 ^e	0.87363
cyclohexane	84.16	280.3	279.6 ^b	2.68 ^c	12.2	1.12 ^f	0.77387
hexane	86.18						0.65507

^a Molecular mass, M ; experimental temperature of fusion, $T_{\text{fus}}^{\text{exp}}$ (this work); literature data of temperature of fusion, $T_{\text{fus}}^{\text{lit}}$; enthalpy of fusion, $\Delta_{\text{fus}}H^{\text{lit}}$; volume expansivity, α^{exp} (this work); isobaric compressibility, κ_T^{exp} (this work); density, $\rho^{298.15,\text{exp}}$ (this work). ^b Average values from NIST. ^c Ref 17. ^d Ref 18. ^e Ref 19. ^f Ref 20.

densities and excess molar volumes, V_{m}^{E} , with benzene and cyclohexane.

Experimental Section

Materials. Pyrrole was from Acros Organics (CAS No. 109-97-7, > 99 %) and was distilled before every measurement. The other chemicals were as follows: benzene (CAS No. 71-43-2, Fluka, > 99.5 %), cyclohexane (CAS No. 110-82-7, Sigma-Aldrich, 99.5 %), and hexane (CAS No. 110-54-3, Sigma-Aldrich, 99 %). The solvent purities are in mass fraction. All solvents were fractionally distilled over different drying reagents until the mass fraction purity was better than 99.8 % and were stored over freshly activated molecular sieves of type 4A (Union Carbide). All compounds were checked by gas-liquid chromatography (GLC) analysis, and no significant impurities were found. The physicochemical characterization of substances is presented in Table 1.

Phase Equilibria Measurements. Solubilities have been determined using a dynamic method that has been described in detail previously.²¹ Appropriate mixtures of pyrrole and solvent placed into a Pyrex glass cell were heated very slowly (less than 2 K·h⁻¹ near the equilibrium temperature) and stirred continuously. The sample was placed in a glass thermostat filled with water or acetone with dry ice. The temperature of the liquid bath was varied slowly until one phase was obtained. The two phase disappearance temperatures in the liquid phase were detected visually during an increasing temperature regime. The temperature was measured with an electronic thermometer P550 (DOSTMANN electronic GmbH) with the probe totally immersed in the thermostating liquid. The thermometer was calibrated on the basis of ITS-90. Mixtures were prepared by mass, and the uncertainty was estimated to be better than ± 0.0002 and ± 0.1 K in the mole fraction and temperature, respectively. The results of the SLE/LLE measurements for the binary systems of {pyrrole (1) + benzene, cyclohexane, or hexane (2)} are presented in Tables 2 to 4. The tables include the direct experimental results of the SLE/LLE temperatures, T^{SLE} or T^{LLE} versus x_1 , the mole fraction of the pyrrole at the equilibrium temperatures for the investigated systems.

Density Measurements. The densities of all of the chemicals and their mixtures were measured using an Anton Paar GmbH 4500 vibrating-tube densimeter (Graz, Austria), thermostatted at different temperatures. Two integrated Pt 100 platinum thermometers provided good precision in temperature control internally ($T \pm 0.01$ K). The densimeter includes an automatic correction for the viscosity of the sample. The apparatus is precise to within $1 \cdot 10^{-5}$ g·cm⁻³, and the uncertainty of the measurements was estimated to be better than $\pm 1 \cdot 10^{-5}$ g·cm⁻³. The densimeter's calibration was performed at atmospheric pressure using doubly distilled and degassed water, specially purified benzene (CHEMIPAN, Poland 0.999), and dried air. Mixtures were prepared by weighing, the uncertainty in mole fraction being estimated as less than $5 \cdot 10^{-4}$. All weighing

Table 2. Experimental SLE Data for the {Pyrrole (1) + Benzene (2)} Binary System: the Mole Fraction, x_1 ; Temperature, T^{SLE} ; and the Activity Coefficient of the Solute, γ_1

x_1	T^{SLE}/K	γ_1	x_1	T^{SLE}/K	γ_1
1.0000	249.6	1.00	0.6714	247.3 ^a	1.77
0.9635	247.2	1.00	0.6196	251.0 ^a	1.64
0.9431	246.1	1.02	0.6047	251.8 ^a	1.60
0.8881	243.5	0.98	0.5386	256.2 ^a	1.49
0.8474	241.5	0.97	0.4461	260.9 ^a	1.35
0.8247	240.1	1.01	0.4320	261.4 ^a	1.33
0.8166	238.6	1.06	0.3806	263.9 ^a	1.27
0.7899	238.1	1.06	0.3212	266.3 ^a	1.21
0.7580	238.2 ^a	2.00	0.2673	268.3 ^a	1.16
0.7343	241.3 ^a	1.94	0.2286	269.8 ^a	1.13
0.7086	243.9 ^a	1.87	0.1704	272.0 ^a	1.09
0.6886	245.5 ^a	1.80	0.0000	278.6 ^{a,b}	1.00

^a Second liquidus curve. ^b The results are, for example, (278.6 \pm 0.1) K.

Table 3. Experimental SLE and LLE Data for the {Pyrrole (1) + Cyclohexane (2)} Binary System: the Mole Fraction, x_1 ; and Temperature, T^{SLE}

x_1	T^{SLE}/K	T^{LLE}/K	x_1	T^{SLE}/K	T^{LLE}/K
1	249.7		0.5828	270.0 ^a	286.1
0.9903	249.3		0.5457	270.0 ^a	286.4
0.9660	247.9		0.5153	270.0 ^a	286.5
0.9647	248.2		0.4835	270.0 ^a	286.8
0.9490	247.8		0.4514	270.0 ^a	286.9
0.9304	246.7		0.4235	270.0 ^a	287.0
0.9272	247.0 ^a		0.3923	270.0 ^a	287.1
0.9084	251.5 ^a		0.3654	270.0 ^a	287.0
0.9056	256.0 ^a		0.3392	270.0 ^a	286.9
0.8911	258.9 ^a		0.3237	270.0 ^a	286.9
0.8807	261.0 ^a		0.2916	270.0 ^a	286.7
0.8690	265.2 ^a		0.2551	270.0 ^a	286.4
0.8573	265.9 ^a		0.2247	270.0 ^a	286.3
0.8505	268.2 ^a		0.2007	270.0 ^a	285.9
0.8338	269.2 ^a		0.1818	270.0 ^a	285.4
0.8304	269.4 ^a		0.1622	270.0 ^a	285.1
0.7944	270.0 ^a	273.8	0.1384	270.0 ^a	284.8
0.7742	270.0 ^a	275.7	0.1125	270.0 ^a	284.2
0.7633	270.0 ^a	277.4	0.0784	270.0 ^a	282.1
0.7428	270.0 ^a	279.1	0.0606	270.0 ^a	279.5 ^c
0.7234	270.0 ^a	280.6	0.0420	271.3 ^a	
0.7163	270.0 ^a	281.7	0.0340	274.6 ^a	
0.6696	270.0 ^a	284.1	0.0202	276.6 ^a	
0.6165	270.0 ^a	285.2	0	280.0 ^{a,b}	

^a Second liquidus curve. ^b The results are, for example, (280.0 \pm 0.1) K. ^c The results are, for example, (279.5 \pm 0.1) K.

involved in the experimental work was carried out using a Mettler Toledo AB 204-S balance, with a precision of $\pm 1 \cdot 10^{-4}$ g. The uncertainty of the excess molar volumes depends on the uncertainties of the density measurements and can be assumed as ± 0.001 cm³·mol⁻¹. The densities of pyrrole and hydrocarbons are shown with other physicochemical properties in Table 1.

For the second part of this work the Anton Paar density measuring cell for high pressures and high temperatures (DMA 512P) and the mPDS 2000 evaluation unit were used for

Table 4. Experimental LLE Data for the {Pyrrole (1) + Hexane (2)} Binary System: the Mole Fraction, x_1 ; and Temperature, T^{LLE}

x_1	T^{LLE}/K	x_1	T^{LLE}/K
0.9070	274.1	0.4234	313.9
0.8925	279.4	0.3935	313.6
0.8605	289.1	0.3657	313.1
0.8240	298.0	0.3363	312.3
0.7948	303.0	0.2972	310.8
0.7682	306.6	0.2549	308.2
0.7393	308.5	0.2122	304.4
0.6950	311.6	0.1702	299.4
0.6408	314.0	0.1373	294.2
0.5857	314.2	0.1070	286.9
0.5390	314.2	0.0869	282.8
0.5008	314.2	0.0627	269.0
0.4678	314.2	0.0351	252.7 ^a
0.4261	313.9		

^a The results are, for example, (252.7 ± 0.1) K.

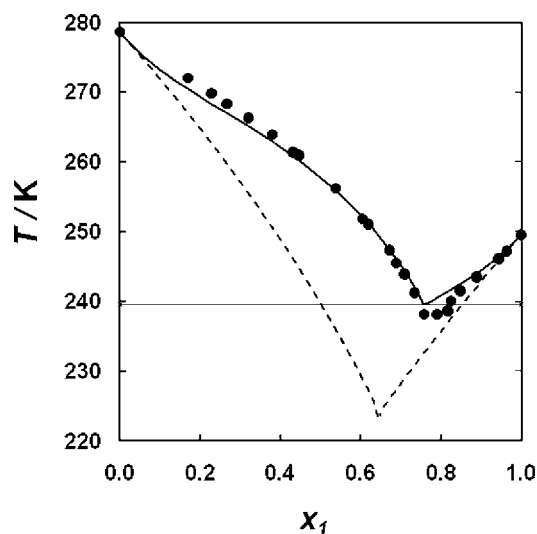


Figure 1. SLE diagram of the binary system {pyrrole (1) + benzene (2)}: ●, experimental points; solid line, calculated by the nonrandom two-liquid (NRTL) equation; dashed line, ideal solubility curve.

measurements of the densities of pure pyrrole at different pressures. This type of densimeter is applicable over the temperature and pressure ranges of (263 to 423) K and (0 to 70) MPa, respectively. The density of the sample is determined by measuring the oscillation period of the U-shaped tube made from Hastelloy C-256 stainless steel. The procedure and the schematic diagram of the apparatus were presented by our group earlier.²²

Results and Discussion

Phase Equilibria. The experimental data of SLE/LLE of the measured binary systems of pyrrole are shown in Figures 1, 2, and 3. The simple eutectic system with complete miscibility in the liquid phase was observed for pyrrole with benzene. This result is similar to (1*H*-imidazole, 1-methyl-1*H*-imidazole, and 2-methyl-1*H*-imidazole + benzene) binary systems.⁷ It can be explained by the possible π - π interaction between two aromatic rings of pyrrole and benzene.

The immiscibility with upper critical solution temperatures (UCSTs) were observed for cyclohexane and hexane (see Figures 2 and 3). For the cyclohexane the solubility is better than in hexane, and the UCSTs are (285.2 and 314.2) K, respectively. The area of the immiscibility is lower for the cyclohexane than for hexane. In fact, this is typical solution behavior, observed for pyrrole with alkanes, which was shown

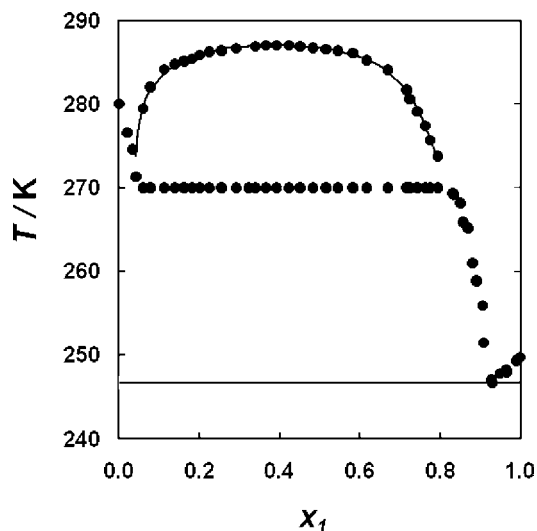


Figure 2. SLE and LLE diagram of the binary system {pyrrole (1) + cyclohexane (2)}: ●, experimental points; solid line, calculated by the NRTL equation.

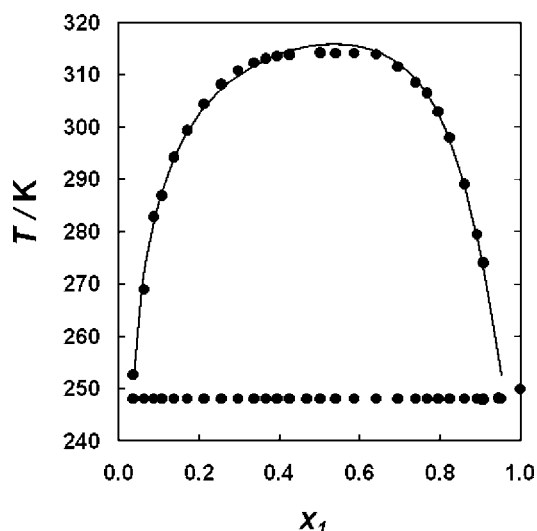


Figure 3. SLE and LLE diagram of the binary system {pyrrole (1) + hexane (2)}: ●, experimental points; solid line, calculated by the NRTL equation.

earlier in the mixtures with hexadecane.^{5,6} Also, 1*H*-imidazole and 2-methyl-1*H*-imidazole revealed SLE with the immiscibility in the liquid phase in the systems with cyclohexane and hexane.⁷

Figure 1 shows two experimental liquidus curves of pyrrole in benzene and benzene in pyrrole. The observed experimental eutectic point is shifted to the higher pyrrole mole fraction: $x_{1,e} = 0.7742$, $T_{1,e} = 237.1$ K. The eutectic point coming from the correlation with the NRTL equation is: $x_{1,e} = 0.7589$, $T_{1,e} = 239.6$ K. The eutectic points for two other investigated systems are shifted to the solvent-rich phase. Below the eutectic temperature we assume the immiscibility of two solid phases.

Packing effects, conformational changes, and interstitial accommodation of the investigated molecules in the binary mixtures are difficult to categorize. All of these effects and the interactions have the influence on phase equilibria and excess molar volumes, measured in this work.

Solid-Liquid and Liquid-Liquid Phase Equilibria Correlation. For the correlation of the solubility of pyrrole in benzene and the calculation of the solute activity coefficients γ_1 , the Wilson²³ and the NRTL equation²⁴ were chosen. As a measure of the reliability of the correlations, the root-mean-

Table 5. Correlation of the SLE Data by Means of the NRTL Equation: Parameters and Temperature Standard Deviation, σ_T /K, in the {Pyrrole (1) + Benzene (2)} Binary System

system	Wilson ($g_{12} - g_{22}$)/J·mol ⁻¹		NRTL ($g_{21} - g_{11}$)/J·mol ⁻¹				
	$\Delta\lambda_{12}$ J·mol ⁻¹	$\Delta\lambda_{21}$ J·mol ⁻¹	σ_T K	α	$(g_{12} - g_{22})$ J·mol ⁻¹	$(g_{21} - g_{11})$ J·mol ⁻¹	σ_T K
benzene	200.01	2333.11	1.34	0.7	2489.88	1495.69	1.28

Table 6. Correlation of the LLE Data by Means of the NRTL Equation: Parameters ($g_{12} - g_{22} = c_{12} + b_{12}T + a_{12}T^2$) and ($g_{21} - g_{11} = c_{21} + b_{21}T + a_{21}T^2$) and the Mole Fraction Deviations σ_x^a

system	$(g_{12} - g_{22})$ /J·mol ⁻¹			$(g_{21} - g_{11})$ /J·mol ⁻¹			σ_x
	a_{12}	b_{12}	c_{12}	a_{21}	b_{21}	c_{12}	
cyclohexane	13.661	-7592.5	1052963	-29.120	16073	-2208000	0.0073
hexane	1.3572	-759.81	108667	-1.5009	805.81	-103248	0.0285

^a Parameter $\alpha = 0.1$ in the {pyrrole (1) + cyclohexane or hexane (2)} binary system.

square deviation of temperature, σ_T /K, has been calculated according to the following definition:

$$\sigma_T = \left\{ \sum_{i=1}^n \frac{(T_{\text{exp},i} - T_{\text{calc},i})^2}{n-2} \right\}^{1/2} \quad (1)$$

where n is the number of experimental points. The values of the parameters and the corresponding root-mean-square deviations of temperature are listed in Table 5. The resulting curve calculated with the NRTL equation is presented together with the experimental points in Figure 1. The solubility of pyrrole in benzene is lower than the ideal solubility ($\gamma_1 > 1$).

The LLE of the systems {pyrrole (1) + cyclohexane or hexane (2)} was correlated with the NRTL model. The equations were described by us earlier.¹⁰ The NRTL α parameter was set to a value of $\alpha = 0.1$, which has given the best results of the correlations.

For LLE, the temperature-dependent model adjustable parameters ($g_{12} - g_{22} = c_{12} + b_{12}T + a_{12}T^2$) and ($g_{21} - g_{11} = c_{21} + b_{21}T + a_{21}T^2$) were found by minimization of the objective function, OF:

$$\text{OF} = \sum_{i=1}^n [(\Delta x_1)_i^2 + (\Delta x_1^*)_i^2] \quad (2)$$

where n is the number of experimental points and Δx_1 and Δx_1^* are the differences of calculated and experimental mole fraction of two liquid phases in equilibrium, defined as

$$\Delta x_1 = x_{\text{calc}} - x_{\text{exp}} \quad (3)$$

The root-mean-square deviation of mole fraction for the LLE calculations was defined as follows:

$$\sigma_x = \left(\frac{\sum_{i=1}^n (\Delta x_1)_i^2 + \sum_{i=1}^n (\Delta x_1^*)_i^2}{2n-2} \right)^{1/2} \quad (4)$$

The results of the correlations and values of model parameters and the corresponding standard deviations are given in Table 6. For the systems presented in this work the average root-mean square deviation σ_x equals 0.0018. The results of the correlations are presented in Figures 2 and 3.

Effect of Temperature on Density. The experimental density, ρ , versus composition data of {pyrrole (1) + benzene or cyclohexane (2)} mixtures at different temperatures are listed in Tables 7 and 8. The densities for the system {pyrrole (1) + hexane (2)} supposed to be measured in temperatures higher than $T_{\text{UCST}} = 314.2$ K, which can provide high experimental error (problem with two phases in the syringe at room temperature and with injection to the apparatus). This was the reason that the experimental densities and excess molar volumes for the mixture of {pyrrole (1) + hexane (2)} were not determined.

As usual, density decreases with increasing temperature for pure substances and for the mixtures. We found no previous data in binary systems as a function of temperature for comparison. A second-order polynomial was found to satisfactorily correlate the change of density with temperature for pure substances:

$$\rho = a_2 T^2 + a_1 T + a_0 \quad (5)$$

where T is for the absolute temperature and a_2 , a_1 , and a_0 refer to the fit coefficients. Fit parameters are listed in Table 9.

Experimental densities at ambient pressure investigated in this work are shown in Figures 1S and 2S in the Supporting Information (SI) for benzene and cyclohexane binary systems, respectively. The linear correlation of the experimental points as a function of temperature in binary mixtures is presented. The obtained parameters are shown in Table 1S in the SI.

Effect of Composition on Density. The densities are higher for pyrrole than for benzene or cyclohexane and decrease with increasing solvent content. The character of changes is presented in Figures 3S and 4S in the SI for benzene and cyclohexane mixtures, respectively. Solid lines were calculated with the polynomial. The parameters of correlation are shown in Table 2S in the SI.

Experimental excess molar volumes V_m^E data of {pyrrole (1) + benzene or cyclohexane (2)} are recorded in Tables 7 and 8. The data were calculated by smoothing the Redlich–Kister equation:

$$V_m^E/(\text{cm}^3 \cdot \text{mol}^{-1}) = x_1(1-x_1) \sum_{i=1}^4 A_i(T)(2x_1-1)^{i-1} \quad (6)$$

with temperature dependence parameters

$$A_i = a_i + b_i T \quad (7)$$

Table 7. Experimental Density, ρ ; Excess Molar Volume, V_m^E ; Volume Expansivity, α ; and Excess Volume Expansivity, α^E , for the Binary System {Pyrrole (1) + Benzene (2)}

x_1	T/K				
	298.15	308.15	318.15	328.15	338.15
	$\rho/\text{g}\cdot\text{cm}^{-3}$				
1.0000	0.96554	0.95683	0.94803	0.93914	0.93013
0.9790	0.96365	0.95492	0.94608	0.93717	0.92812
0.9214	0.95896	0.95013	0.94121	0.93219	0.92304
0.8732	0.95472	0.94581	0.93680	0.92770	0.91846
0.8207	0.95033	0.94134	0.93226	0.92307	0.91374
0.7371	0.94299	0.93385	0.92462	0.91529	0.90582
0.6693	0.93698	0.92773	0.91838	0.90892	0.89934
0.5973	0.93057	0.92115	0.91166	0.90207	0.89235
0.5030	0.92204	0.91244	0.90277	0.89298	0.88308
0.3916	0.91183	0.90201	0.89211	0.88208	0.87195
0.3142	0.90435	0.89436	0.88428	0.87410	0.86391
0.2144	0.89489	0.88468	0.87436	0.86395	0.85341
0.1287	0.88660	0.87617	0.86566	0.85506	0.84434
0.0447	0.87811	0.86749	0.85679	0.84600	0.83510
0.0000	0.87363	0.86291	0.85212	0.84124	0.83026
	$V_m^E/\text{cm}^3\cdot\text{mol}^{-1}$				
1.0000	0.000	0.000	0.000	0.000	0.000
0.9790	-0.042	-0.046	-0.048	-0.052	-0.055
0.9214	-0.186	-0.198	-0.210	-0.222	-0.233
0.8732	-0.275	-0.292	-0.310	-0.328	-0.345
0.8207	-0.381	-0.405	-0.430	-0.455	-0.479
0.7371	-0.504	-0.535	-0.568	-0.602	-0.636
0.6693	-0.581	-0.619	-0.658	-0.697	-0.737
0.5973	-0.643	-0.682	-0.724	-0.768	-0.812
0.5030	-0.684	-0.726	-0.771	-0.816	-0.864
0.3916	-0.676	-0.718	-0.762	-0.805	-0.851
0.3142	-0.605	-0.644	-0.683	-0.723	-0.775
0.2144	-0.493	-0.524	-0.553	-0.584	-0.615
0.1287	-0.343	-0.363	-0.382	-0.403	-0.423
0.0447	-0.127	-0.134	-0.141	-0.148	-0.154
0.0000	0.000	0.000	0.000	0.000	0.000
	$10^4\cdot\alpha/\text{K}^{-1}$				
1.0000	9.0	9.1	9.3	9.5	9.7
0.9790	9.0	9.2	9.4	9.6	9.8
0.9214	9.1	9.3	9.5	9.7	9.9
0.8732	9.2	9.5	9.7	9.9	10.1
0.8207	9.4	9.6	9.8	10.0	10.2
0.7371	9.6	9.8	10.0	10.3	10.5
0.6693	9.8	10.0	10.2	10.5	10.7
0.5973	10.0	10.2	10.5	10.7	11.0
0.5030	10.3	10.5	10.8	11.0	11.3
0.3916	10.7	10.9	11.2	11.4	11.7
0.3142	11.0	11.2	11.5	11.7	12.0
0.2144	11.3	11.6	11.8	12.1	12.4
0.1287	11.7	11.9	12.2	12.5	12.7
0.0447	12.0	12.3	12.5	12.8	13.1
0.0000	12.2	12.5	12.7	13.0	13.3
	$10^4\cdot\alpha^E/\text{K}^{-1}$				
1.0000	0.00	0.00	0.00	0.00	0.00
0.9790	-0.04	-0.04	-0.04	-0.04	-0.04
0.9214	-0.15	-0.14	-0.14	-0.13	-0.13
0.8732	-0.22	-0.22	-0.21	-0.20	-0.20
0.8207	-0.29	-0.28	-0.28	-0.27	-0.26
0.7371	-0.38	-0.37	-0.36	-0.35	-0.34
0.6693	-0.43	-0.42	-0.41	-0.40	-0.38
0.5973	-0.46	-0.45	-0.44	-0.43	-0.41
0.5030	-0.48	-0.46	-0.45	-0.44	-0.42
0.3916	-0.45	-0.43	-0.42	-0.41	-0.39
0.3142	-0.40	-0.39	-0.38	-0.36	-0.35
0.2144	-0.31	-0.30	-0.29	-0.28	-0.27
0.1287	-0.20	-0.20	-0.19	-0.18	-0.18
0.0447	-0.08	-0.07	-0.07	-0.07	-0.07
0.0000	0.00	0.00	0.00	0.00	0.00

where x_1 is the mole fraction of the pyrrole, V_m^E is the excess molar volume, and i is the number of parameters. The values of the parameters (A_i) for V_m^E have been determined using a method of least-squares. The fit temperature dependence of the Redlich–Kister parameters are summarized in Table 10. The

values of V_m^E as well as the Redlich–Kister fits are plotted in Figures 4 and 5 for the concentration dependence of the excess molar volume for benzene and cyclohexane, respectively. The graphs of V_m^E indicate that both mixtures exhibit negative deviations from ideality over the entire composition range. The

Table 8. Experimental Density, ρ ; Excess Molar Volume, V_m^E ; Volume Expansivity, α ; and Excess Volume Expansivity, α^E , for the Binary Systems {Pyrrole (1) + Cyclohexane (2)}

x_1	T/K				
	298.15	308.15	318.15	328.15	338.15
	$\rho/\text{g}\cdot\text{cm}^{-3}$				
1.0000	0.96554	0.95683	0.94803	0.93914	0.93013
0.9424	0.95379	0.94505	0.93621	0.92725	0.91818
0.8824	0.94141	0.93259	0.92370	0.91469	0.90555
0.8376	0.93214	0.92329	0.91435	0.90529	0.89610
0.7610	0.91678	0.90783	0.89879	0.88965	0.88041
0.7183	0.90828	0.89928	0.89020	0.88103	0.87179
0.6712	0.89856	0.88948	0.88032	0.87017	0.86168
0.6032	0.88476	0.87558	0.86633	0.85697	0.84756
0.5058	0.86613	0.85680	0.84740	0.83791	0.82838
0.4446	0.85423	0.84482	0.83534	0.82581	0.81630
0.3549	0.83714	0.82763	0.81803	0.80835	0.79862
0.2637	0.81991	0.81032	0.80064	0.79086	0.78096
0.1864	0.80548	0.79587	0.78614	0.77630	0.76632
0.1409	0.79778	0.78817	0.77844	0.76858	0.75860
0.0749	0.78603	0.77643	0.76672	0.75688	0.74691
0.0000	0.77387	0.76438	0.75477	0.74504	0.73518
	$V_m^E/\text{cm}^3\cdot\text{mol}^{-1}$				
1.0000	0.000	0.000	0.000	0.000	0.000
0.9424	-0.376	-0.390	-0.404	-0.416	-0.430
0.8824	-0.705	-0.728	-0.754	-0.780	-0.806
0.8376	-0.913	-0.944	-0.977	-1.010	-1.044
0.7610	-1.239	-1.278	-1.320	-1.364	-1.413
0.7183	-1.386	-1.429	-1.476	-1.526	-1.585
0.6712	-1.486	-1.529	-1.576	-1.541	-1.681
0.6032	-1.581	-1.623	-1.671	-1.722	-1.783
0.5058	-1.691	-1.729	-1.773	-1.822	-1.884
0.4446	-1.656	-1.689	-1.728	-1.777	-1.845
0.3549	-1.519	-1.542	-1.570	-1.604	-1.650
0.2637	-1.242	-1.253	-1.268	-1.287	-1.308
0.1864	-0.899	-0.901	-0.904	-0.908	-0.911
0.1409	-0.741	-0.741	-0.740	-0.738	-0.738
0.0749	-0.368	-0.361	-0.355	-0.347	-0.338
0.0000	0.000	0.000	0.000	0.000	0.000
	$10^4\cdot\alpha/\text{K}^{-1}$				
1.0000	9.0	9.1	9.3	9.5	9.7
0.9424	9.1	9.3	9.5	9.7	10.0
0.8824	9.3	9.5	9.7	10.0	10.2
0.8376	9.4	9.6	9.9	10.1	10.4
0.7610	9.6	9.9	10.1	10.4	10.6
0.7183	9.8	10.0	10.3	10.5	10.8
0.6712	9.9	10.2	10.5	10.7	11.0
0.6032	10.2	10.4	10.7	11.0	11.3
0.5058	10.6	10.8	11.1	11.4	11.7
0.4446	10.8	11.1	11.4	11.7	12.0
0.3549	11.2	11.5	11.8	12.1	12.4
0.2637	11.6	11.9	12.2	12.5	12.8
0.1864	11.8	12.1	12.4	12.8	13.1
0.1409	12.0	12.3	12.6	12.9	13.2
0.0749	12.1	12.4	12.7	13.1	13.4
0	12.2	12.5	12.8	13.1	13.5
	$10^4\cdot\alpha^E/\text{K}^{-1}$				
1	0.00	0.00	0.00	0.00	0.00
0.9424	-1.15	-1.10	-1.06	-1.01	-0.97
0.8824	-2.26	-2.17	-2.09	-2.00	-1.92
0.8376	-2.96	-2.86	-2.75	-2.64	-2.52
0.7610	-3.85	-3.71	-3.57	-3.43	-3.28
0.7183	-4.14	-3.99	-3.84	-3.68	-3.53
0.6712	-4.28	-4.13	-3.97	-3.80	-3.64
0.6032	-4.17	-4.01	-3.85	-3.68	-3.51
0.5058	-3.42	-3.28	-3.13	-2.97	-2.82
0.4446	-2.69	-2.56	-2.43	-2.29	-2.15
0.3549	-1.42	-1.32	-1.22	-1.12	-1.01
0.2637	-0.17	-0.10	-0.03	0.03	0.10
0.1864	0.62	0.66	0.69	0.73	0.77
0.1409	0.87	0.89	0.91	0.93	0.96
0.0749	0.82	0.83	0.83	0.84	0.84
0	0.00	0.00	0.00	0.00	0.00

minimum of V_m^E is $(-0.68$ and $-1.69)$ $\text{cm}^3\cdot\text{mol}^{-1}$ at $x_1 = 0.50$ (at $T = 298.15$ K) for benzene and cyclohexane, respectively.

With the increasing temperature the minimum of V_m^E shifts to the higher values of V_m^E . The excess molar volume data become

Table 9. Fit Parameters a_0 , a_1 , and a_2 for the Empirical Correlation of the Density as a Function of Temperature for Pure Substances^a

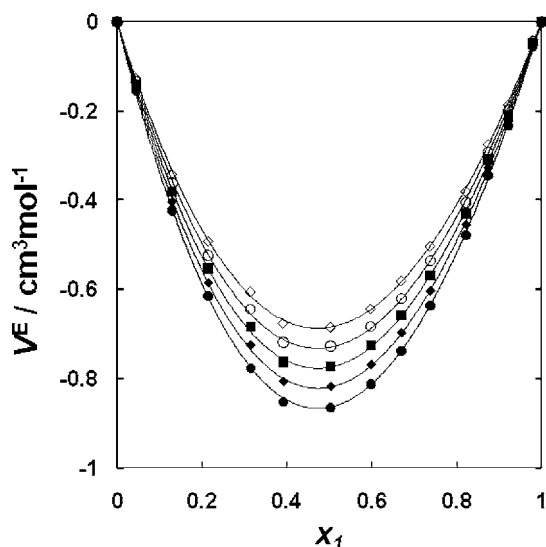
compound	$10^7 \cdot a_2$ $\text{g} \cdot \text{cm}^{-3} \cdot \text{K}^{-2}$	$10^4 \cdot a_1$ $\text{g} \cdot \text{cm}^{-3} \cdot \text{K}^{-1}$	a_0 $\text{g} \cdot \text{cm}^{-3}$	R^2
pyrrole	-4.93	-5.71	1.1797	0.9999
benzene	-4.36	-8.07	1.1529	0.9999
cyclohexane	6.14	-5.76	1.0003	0.9999

^a $\rho/(\text{g} \cdot \text{cm}^{-3}) = a_2(T/\text{K})^2 + a_1(T/\text{K}) + a_0$ (in the range of experimental data).

Table 10. Coefficients of the Redlich–Kister Equation^a for the Correlation of the Excess Molar Volume, $V_m^E/(\text{cm}^3 \cdot \text{mol}^{-1})$, with Temperature-Dependent Parameters^b

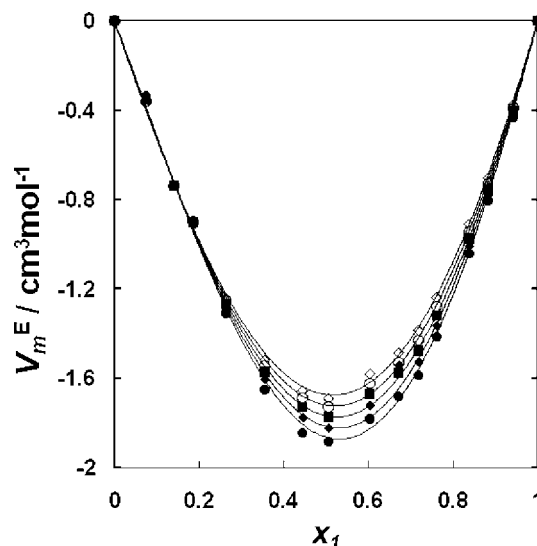
i	a_i	$10^2 \cdot b_i$
Pyrrole (1) + Benzene (2)		
1	2.610	-1.794
2	0.205	-0.170
$\sigma^c = 0.0057 \text{ cm}^3 \cdot \text{mol}^{-1}$		
Pyrrole (1) + Cyclohexane (2)		
1	-1.006	-1.907
2	-4.253	1.591
3	-3.883	1.528
$\sigma^c = 0.027 \text{ cm}^3 \cdot \text{mol}^{-1}$		

^a $V_m^E/(\text{cm}^3 \cdot \text{mol}^{-1}) = x_1(1 - x_1) \sum_{i=1}^3 A_i(T)(2x_1 - 1)^{i-1}$. ^b $A_i = a_i + b_i T$.
^c $\sigma = [1/N \sum (V_{\text{exp}}^E - V_{\text{calc}}^E)^2]^{1/2}$.

**Figure 4.** Excess molar volume V_m^E versus x_1 for the {pyrrole (1) + benzene (2)} binary system at different temperatures: ●, 298.15 K; ◆, 308.15 K; ■, 318.15 K; ○, 328.15 K; ◇, 338.15 K. Solid lines represent the Redlich–Kister equation.

more negative in the following order: cyclohexane < benzene. The higher negative deviations from ideality are observed for cyclohexane. However, it cannot be a result of a stronger interaction of pyrrole with cyclohexane. The strength of the intermolecular interaction coming from the phase equilibria is opposite. The molecular size and shape of the components and the packing effect are here the equally important factors. The free volume effect, which depends on differences in the characteristic pressures and temperatures of the components, makes also a negative contribution. Packing effects or conformational changes of the molecules in the mixtures are more important in the mixture with cyclohexane. Also, the interstitial accommodation and the effect of the condensation give further negative contributions in the mixture with cyclohexane.

From the density–temperature dependence one can calculate the volume expansivity (coefficient of thermal expansion), α ,

**Figure 5.** Excess molar volume V_m^E versus x_1 for the {pyrrole (1) + cyclohexane (2)} binary system at different temperatures: ●, 298.15 K; ◆, 308.15 K; ■, 318.15 K; ○, 328.15 K; ◇, 338.15 K. Solid lines represent the Redlich–Kister equation.

defined as:

$$\alpha = \frac{1}{V} \left(\frac{\partial V}{\partial T} \right)_p = -\frac{1}{\rho} \left(\frac{\partial \rho}{\partial T} \right)_p \quad (8)$$

where the subscript p indicates constant pressure. If one considers a plot of ρ versus T to be linear, then the magnitude of α increases with increasing temperature. Using the eqs 6 to 8, the volume expansivity can be presented in a function of the composition and temperature. The results of our analysis for pure substances and their mixtures are listed in Tables 7 and 8. The errors of derived values of parameters calculated through the statistical analysis depend significantly on the form of an equation chosen to represent density as a function of temperature at constant pressure. As a result, the increasing volume expansivity with increasing temperature was observed. This is typical behavior for fluids in general. Plots of volume expansivity α of the binary {pyrrole (1) + benzene, or cyclohexane (2)} systems against mole fraction x_1 at different temperatures (298.15, 308.15, 318.15, 328.15, and 338.15) K are shown in Figures 5S and 6S in the SI for benzene and cyclohexane, respectively. The trends of the volume expansivity with the composition of the mixtures are the same for two solvents, for which the parameter α decreases with an increase of the mole fraction of pyrrole. This decrease is nonlinear, being less regular at low mole fractions of the pyrrole. Thus, these solutions reveal the volumetric properties typical for mixtures of two organic compounds.

Next the corresponding excess function was determined. The excess volume expansivity was calculated by the equation:²²

$$\alpha^E = \alpha - \varphi_1^{\text{id}} \alpha_1 - \varphi_2^{\text{id}} \alpha_2 \quad (9)$$

where φ_i^{id} is an ideal volume fraction given by the following relation:

$$\varphi_1^{\text{id}} = \frac{x_1 V_{m1}}{x_1 V_{m1} + x_2 V_{m2}} \quad (10)$$

in which V_{mi} stands for a molar volume for a pure component i .

Table 11. Isothermal ($T = 298.15$ K) Density Measurements for Pyrrole as a Function of Pressure^a

p/MPa	$\rho/\text{g}\cdot\text{cm}^{-3}$
0.1	0.96554
0.5	0.96571
1	0.96600
1.5	0.96630
2	0.96659
2.5	0.96690
3	0.96719
4	0.96777
5	0.96835

^a $\rho/(\text{g}\cdot\text{cm}^{-3}) = a + bp$, where $a = 0.9654 \text{ g}\cdot\text{cm}^{-3}$ and $b = 0.588\cdot 10^{-3} \text{ g}\cdot\text{cm}^{-3}\cdot\text{MPa}^{-1}$.

Table 12. Characteristic Parameters of Pure Components: Volume V^* , Temperature T^* , Pressure P^* , Reduced Volume \tilde{v} , and Interaction Parameters, χ_{12} , for Pyrrole Binary Systems at $T/\text{K} = 298.15$

component	V^* $\text{cm}^3\cdot\text{mol}^{-1}$	T^* K	P^* $\text{J}\cdot\text{cm}^{-3}$	\tilde{v}	χ_{12} $\text{J}\cdot\text{mol}^{-3}$
pyrrole	56.69	5567	661	1.226	
benzene	69.24	4715	628	1.291	-56.3
cyclohexane	84.27	4715	541	1.291	-121

Typical concentration dependencies of excess expansivity are given in Figure 7S in the SI for the {pyrrole (1) + benzene (2)} binary system. This mixture reveals a minimum of α^E with the absolute minimum value at $x_1 = 0.50$ (-0.48 K^{-1} at 298.15 K). The curves are symmetrical, and the values increase (are less negative) with an increase of temperature.

A different picture is observed for the system {pyrrole (1) + cyclohexane (2)} with the maximum located at $x_1 = 0.14$ and minimum located at $x_1 = 0.67$ (see Figure 8S in the SI). Thus, the specific interaction between two dissimilar molecules increases for the larger mole concentration of pyrrole. The excess expansivity increases with an increase of temperature.

Prigogine–Flory–Paterson (PFP) Model. The theory of Flory and co-workers^{25–27} has been useful in predicting and correlating the thermodynamic properties of binary mixtures of polar and nonpolar molecules. The PFP model has been applied to the mixtures investigated in this work using the same procedure and formulas as published before.²⁸ The interchange parameter χ_{12} which minimized V_m^E experimental data was adjusted and then used to calculate H_m^E in the systems {pyrrole (1) + benzene, or cyclohexane (2)}, using the thermal expansivity, α , and isobaric compressibility, κ_T , of pyrrole measured for this purposes (see Table 1). The values of density of pyrrole as a function of pressure are listed in Table 11. The pure substance characteristic parameters, volume V^* , temperature T^* , pressure P^* , reduced volume \tilde{v} , and the interchange parameter χ_{12} at $T = 298.15$ K are presented in Table 12.

A comparison of the predicted excess molar enthalpy for these two systems shows that predicted H_m^E values for the (pyrrole + benzene) mixture are less negative ($H_{\text{mmin}}^E = -0.85 \text{ kJ}\cdot\text{mol}^{-1}$) than for the (pyrrole + cyclohexane) mixture ($H_{\text{mmin}}^E = -2.1 \text{ kJ}\cdot\text{mol}^{-1}$). The values of predicted H_m^E values are summarized in Table 3S in the SI. The predictive curves of H_m^E are plotted in Figure 9S in the SI. For both solvents the excess molar enthalpies are negative. The negative excess molar enthalpies demonstrate strong interactions between pyrrole and solvents under study. The presented results from phase equilibria demonstrated that pyrrole interacts with cyclohexane (LLE) more weakly than with benzene (SLE) in the solutions. Thus, it should be noted that estimates of excess molar volumes and enthalpies, on the basis of the interchange energy parameter,

obtained from the present analysis of excess molar volumes, may exhibit relatively large deviations from the experimental results (no H_m^E data for pyrrole) due to the importance of contributions from other structural effects and conformational changes in the solution.

Conclusions

The SLE for one and LLE for two new binary (pyrrole + organic solvent) systems were determined. Complete miscibility in the liquid phase was observed with benzene. The experimental data of LLE in binary systems of pyrrole with cyclohexane and hexane demonstrates the miscibility gap in the liquid phase. The existence of the LLE is the evidence that the interaction between the pyrrole and the solvent is not significant. This knowledge was not confirmed by the excess molar volumes and excess molar enthalpy discussion. The impact of different factors on the liquid-phase behavior of pyrrole was discussed.

New data on the densities of pure pyrrole, benzene, cyclohexane, and their binary mixtures were measured. From the density–temperature dependence the excess molar volumes, the volume expansivity, the excess volume expansivity, and the isobaric compressibility were described for the pyrrole mixtures at different temperatures. In this work the negative deviations were observed for excess molar volumes and excess molar enthalpies calculated by the PFP theory. The lower V_m^E of pyrrole with cyclohexane may be explained by possible better packing effects.

The results of the correlations with the second-order polynomial, the Redlich–Kister equation, and PFP theory of density and excess molar volumes were with very low standard deviations.

Supporting Information Available:

Density for the {pyrrole (1) + benzene or cyclohexane (2)} binary systems as a function of temperature at different mole fractions of pyrrole in Figures 1S and 2S and as a function of mole fraction at different temperatures in Figures 3S and 4S. Fit parameters for these systems in Tables 1S and 2S. Plots of volume expansivity and excess volume expansivity in Figures 5S–8S. Excess molar enthalpy in Figure 9S and Table 3S. This material is available free of charge via the Internet at <http://pubs.acs.org>.

Literature Cited

- Wilding, W. V.; Adams, K. L.; Carmichael, A. E.; Hull, J. B.; Jarman, T. C.; Jenkins, K. P.; Marshall, T. L.; Wilson, H. L. Vapor-Liquid equilibrium measurements on Three Binary Mixtures: Difluoromethane/Hydrogen Chloride, cis-1,3-Dichloropropene/trans-1,3-Dichloropropene, and Pyrrole/Water. *J. Chem. Eng. Data* **2002**, *47*, 748–756.
- Rai, N.; Siepmann, J. I. Transferable Potentials for Phase Equilibria. 9. Explicit Hydrogen Description of Benzene and Five-Membered and Six-Membered Heterocyclic Aromatic Compounds. *J. Phys. Chem. B* **2007**, *111*, 10790–10799.
- Kulik, B.; Kruse, S.; Peltó, J. High Pressure Phase Equilibrium Studies of the Pyrrole–Carbon Dioxide Binary System. *J. Supercrit. Fluids* **2008**, *47*, 135–139.
- Thamanavat, K.; Sun, T.; Teja, S. High Pressure Phase Equilibrium in the Carbon Dioxide–Pyrrole System. *Fluid Phase Equilib.* **2009**, *275*, 60–63.
- Hwang, I.-C.; Park, S.-J.; Seo, D.-W.; Han, K.-J. Binary Liquid-Liquid Equilibrium (LLE) for *N*-Methylformamide (NMF) + Hexadecane between (288.15 and 318.15) K and Ternary LLE for Systems of NMF + Heterocyclic Nitrogen Compounds + Hexadecane. *J. Chem. Eng. Data* **2009**, *54*, 78–82.
- Kim, H.-D.; Hwang, I.-C.; Park, S.-J.; Lee, W. (Liquid + Liquid) Equilibrium for (*N,N*-Dimethylformamide (DMF) + Hexadecane) at Temperature Between (298.15 and 313.15) K and Ternary Mixtures of (DMF + Hexadecane) with Either Quinoline, or Pyridine, or Pyrrole, or Aniline, or Indole at $T = 298.15$ K. *J. Chem. Eng. Data* **2010**, *55*, 1266–1270.
- Domańska, U.; Zawadzki, M.; González, J. A. Thermodynamics of Organic Mixtures Containing Amines. X. Phase Equilibria for Binary

- Systems Formed by Imidazoles and Hydrocarbons: Experimental Data and Modelling Using DISQUAC. *J. Chem. Thermodyn.* **2010**, *42*, 545–552.
- (8) Łachwa, J.; Szydłowski, J.; Najdanovic-Visak, V.; Rebelo, L. P. N.; Seddon, K. R.; Nunes da Ponte, M.; Esperanca, J. M. S. S.; Guedes, H. J. R. Evidence for Critical Solution Behavior in Ionic Liquid Solution. *J. Am. Chem. Soc.* **2005**, *127*, 6542–6543.
- (9) Alonso, L.; Arce, A.; Francisco, M.; Soto, A. Phase Behaviour of 1-Methyl-3-octylimidazolium Bis[trifluoromethylsulfonyl]imide with Thiophene and Aliphatic Hydrocarbons: The Influence of *n*-Alkane Chain Length. *Fluid Phase Equilib.* **2008**, *263*, 176–181.
- (10) Domańska, U.; Marciniak, A. Phase Behaviour of 1-Hexyloxymethyl-3-methyl-imidazolium and 1,3-Dihexyloxymethyl-imidazolium Based Ionic Liquids with Alcohols, Water, Ketones and Hydrocarbons: The Effect of Cation and Anion on Solubility. *Fluid Phase Equilib.* **2007**, *260*, 9–18.
- (11) Domańska, U.; Laskowska, M. Measurements of Activity Coefficients at Infinite Dilution of Aliphatic and Aromatic Hydrocarbons, Alcohols, Thiophene, Tetrahydrofuran, MTBE and Water in Ionic Liquid [BMIM][SCN] using GLC. *J. Chem. Thermodyn.* **2009**, *41*, 645–650.
- (12) Domańska, U.; Marciniak, A. Measurements of Activity Coefficients at Infinite Dilution of Aromatic and Aliphatic Hydrocarbons, Alcohols, and Water in the New Ionic Liquid [EMIM][SCN] using GLC. *J. Chem. Thermodyn.* **2008**, *40*, 860–866.
- (13) Domańska, U.; Laskowska, M.; Pobudkowska, A. Phase Equilibria Study of Their Binary Systems (1-Butyl-3-methylimidazolium Thiocyanate Ionic Liquid + Organic solvent, or Water). *J. Phys. Chem. B* **2009**, *113*, 6397–6404.
- (14) Kato, R.; Krummen, M.; Gmehling, J. Measurements and Correlation of Vapor-Liquid Equilibria and Excess Enthalpies of Binary Systems Containing Ionic Liquids and Hydrocarbons. *Fluid Phase Equilib.* **2004**, *224*, 47–54.
- (15) Kato, R.; Gmehling, J. Systems with Ionic Liquids: Measurements of VLE and γ_∞ Data and Prediction of their Thermodynamic Behavior Using Original UNIFAC, mod. UNIFAC(D0) and COSMO-RS(01). *J. Chem. Thermodyn.* **2005**, *37*, 603–619.
- (16) Mokhtarani, B.; Gmehling, J. Vapor-Liquid Equilibria of Ternary Systems with Ionic Liquids Using Headspace Gas Chromatography. *J. Chem. Thermodyn.* **2010**, *42*, 1036–1038.
- (17) Domalski, E. S.; Hearing, E. D. Heat Capacities and Entropies of Organic Compounds in the Condensed Phase. Volume III. *J. Phys. Chem. Ref. Data* **1996**, *25*, 1–525.
- (18) Riddick, J. A.; Bunger, W. B.; Sakano, T. K. Organic Solvents. In *Techniques of Chemistry*, Vol. 2; Weissberger, A., Ed.; Wiley: New York, 1986.
- (19) Matsuo, S.; Van Hook, A. Isothermal Compressibility of C₆H₆, C₆D₆, c-C₆H₁₂, c-C₆D₁₂, and their Mixtures from 0.1 to 35 MPa at 288, 298, and 313 K. *J. Phys. Chem.* **1984**, *88*, 1032–1040.
- (20) Aicart, E.; Tardajos, G.; Diaz Pena, M. Isothermal Compressibility of Cyclohexane + Hexane, Cyclohexane + Heptane, Cyclohexane + Octane, and Cyclohexane + Nonane. *J. Chem. Eng. Data* **1980**, *25*, 145–147.
- (21) Domańska, U. Vapour-Liquid-Solid Equilibrium of Eicosanoic Acid in One- and Two-component Solvents. *Fluid Phase Equilib.* **1986**, *26*, 201–220.
- (22) Goldon, A.; Dąbrowska, K.; Hofman, T. Densities and Excess Volumes of the 1,3-Dimethylimidazolium Methylsulfate + Methanol System at Temperatures from (313.15 to 333.15) K and Pressures from (0.1 to 25) MPa. *J. Chem. Eng. Data* **2007**, *52*, 1830–1837.
- (23) Wilson, G. M. Vapour-Liquid Equilibrium. XI. A new Expression for the Excess Free Energy of Mixing. *J. Am. Chem. Soc.* **1964**, *86*, 127–130.
- (24) Renon, H.; Prausnitz, J. M. Local Composition in Thermodynamic Excess Functions for Liquid Mixtures. *AIChE J.* **1968**, *14*, 135–144.
- (25) Flory, P. J. Statistical Thermodynamics of Liquid Mixtures. *J. Am. Chem. Soc.* **1965**, *87*, 1833–1835.
- (26) Abe, A.; Flory, P. J. The Thermodynamic Properties of Mixtures of Small, Nonpolar Molecules. *J. Am. Chem. Soc.* **1965**, *87*, 1838–1842.
- (27) Orwoll, R. A.; Flory, P. J. Equation of State Parameters for Normal Alkanes. Correlation with Chain Length. *J. Am. Chem. Soc.* **1967**, *89*, 6822–6825.
- (28) Domańska, U.; Pobudkowska, A.; Wiśniewska, A. Solubility and Excess Molar Properties of 1,3-Dimethylimidazolium Methylsulfate, or 1-Butyl-3-methylimidazolium Methylsulfate, or 1-Butyl-3-methylimidazolium Octylsulfate Ionic Liquids With *n*-Alkanes and Alcohols: Analysis in Terms of the PFP and FBT Models. *J. Solution Chem.* **2006**, *35*, 311–334.

Received for review May 20, 2010. Accepted July 14, 2010. This work has been supported by the Warsaw University of Technology.

JE100526J